

G. M. Ye,
D. F. Shen

College of Mechanical Engineering,
Dong Hua University,
Shanghai 201620, P.R.China
E-mail:sdfdu@163.com

Study on Pneumatic Weft Insertion Behaviour in Main Nozzle

Abstract

In this paper, with the aim of analysis, the main nozzle was divided into four part (tubes). This allowed to analyse detailed airflow parameters of each tube, and introduce a method of experiment to test the airflow velocity in the exit nozzle and weft tension in the main nozzle. On the basis of fluid dynamics, the pull force formula of main nozzle on an air jet loom was determined in this paper. The theoretical findings agreed well with the experimental.

Key words: weft insertions, unsteady flow, pull force, main nozzle, testing.

The notations used in this paper are as follows:

- R - gas constant (= 8.314J/molK),
 μ_B - frictional coefficient between the airflow and the tube B wall,
 L_B - length of the cylindrical tube B,
 D_B - inner diameter of cylindrical tube B,
 k - adiabatic coefficient (= 1.4),
 μ_{C2} - frictional coefficient of tube C2,
 L_{C2} - length of tube C2,
 D_{C2} - inner diameter of tube C2,
 T_0 - atmospheric temperature of workshop,
 C_p - specific heat at constant pressure,
 P_T - pressure of main tank,
 T_T - airflow temperature of main tank,
 M_{A2} - mach number of airflow at tube A exit,
 P_{A2} - the pressure of tube A exit,
 T_{A2} - airflow temperature of tube A exit,
 V_{A2} - airflow velocity of tube A exit,
 c_{A2} - sonic velocity of tube A exit,
 ρ_{A2} - airflow density of tube A exit,
 m_{A2} - mass flow of tube A exit,
 P_{A2} - airflow pressure of tube A exit,
 A_{A2} - sectional area of tube A exit,
 ρ_{A2} - airflow density of tube A exit,
 V_{A2} - airflow velocity of tube A exit,
 P_{B2} - airflow pressure of tube B exit,
 A_{B2} - sectional area of tube B exit,
 V_{B2} - airflow velocity of tube B exit,
 ρ_{B2} - airflow density of tube B exit,
 \dot{m}_{B2} - mass flow of tube B exit,
 M_{B1} - airflow Mach number of cylindrical tube B inlet,
 M_{B2} - airflow Mach number at tube B exit,
 P_{C12} - airflow pressure of tube C1 exit,
 A_{C12} - sectional area of tube C1 exit,
 V_{C12} - airflow velocity of tube C1 exit,
 ρ_{C12} - airflow density of tube C1 exit,
 \dot{m}_{C12} - airflow mass flow of tube C1 exit,
 M_{C21} - airflow Mach number of tube C2 inlet,
 T_{C21} - airflow temperature of tube C2 inlet,
 V_{C21} - airflow velocity of tube C2 inlet,

- ρ_{C21} - airflow density of tube C2 inlet,
 c_{C21} - airflow local sonic velocity of tube C2 inlet,
 M_{C22} - airflow Mach number of tube C2 exit,
 T_{C22} - airflow temperature of tube C2 exit,
 V_{C22} - airflow velocity of tube C2 exit,
 ρ_{C22} - airflow density of tube C2 exit,
 P_{C22} - airflow pressure of tube C2 exit,
 c_{C22} - airflow local sonic velocity of tube C2 exit.

Introduction

The air jet loom is popular in the textile industry because of its high productivity, convenient controllability, and wide variety of products manufactured from it fabrics. In order to improve airflow efficiency, many researchers have studied this, using the quantitative analysis method with different paths in the air jet weft insertion of the air jet loom [1-5]. Despite several decades of intensive research, the varieties of friction coefficient values of yarn, nozzle shape and working accuracy of the nozzle continue to make the theoretical arithmetic hard to predict, and so there are always some differences between the calculated and measured values. For this reason, this paper also

employs theoretic analysis and experiment to explain how each parameter of the main nozzle affects the pull force of the airflow on the weft (hereinafter abbreviated as PF).

Structure analysis and calculation of airflow parameters

The structure analysis of main nozzle

The Reynolds number is about 10^6 when the main nozzle of the air jet loom is filled with air [6]. So, the airflow of the air jet weft insertion is turbulent with low pressure, a small quantity flow and a subsonic velocity. Figure 1 shows an example of the main nozzle structure, where A is the nozzle body, B is the nozzle needle, C is the thread tube (it also can be divided into tube C1 and tube C2), D is the weft inlet, a is the airflow inlet, b is the first air chamber, c is the rectifier tank, d is the second air chamber, e is the throat, f is the nozzle needle exit, and g is the weft acceleration zone.

Compressed air flows from the main tank to the main nozzle through airflow inlet a. The first air chamber b is cyclic, the airflow flows along the axis and circles

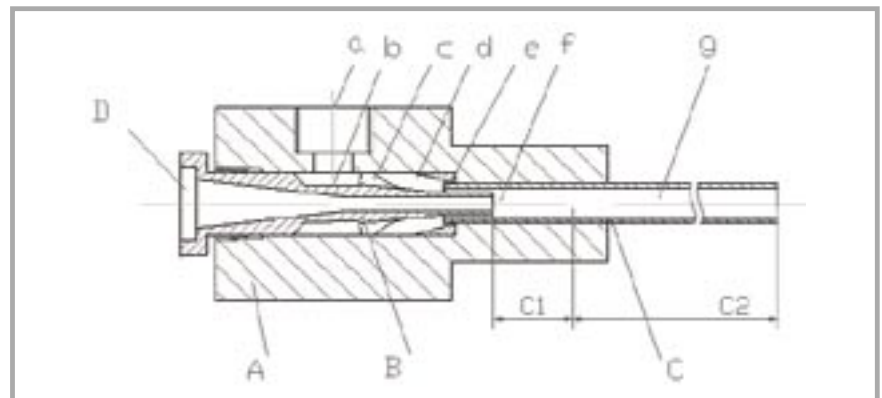


Figure 1. Single channel main nozzle structure, A-nozzle body, B-nozzle needle, C- thread tube, a- airflow inlet, b- first air chamber, c- rectifier tank, d- second air chamber, e- throat, f- nozzle needle exit, g- weft acceleration zone.

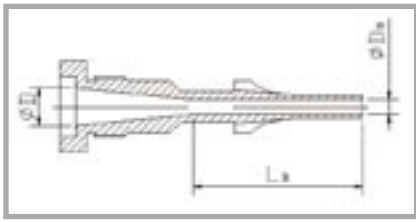


Figure 2. Schematic diagram of main nozzle needle.

when it enters the first air chamber, and a high-speed eddy flow comes into being. Rectifier tank c has many grooves along the circle, the high-speed eddy flow can be adjusted and becomes a direct current when it passes the rectifier tank. The second air chamber d is also cyclic, the airflow can be accelerated and becomes a subsonic axial flow. The airflow reaches sonic velocity when it passes throat e. Thread tube C is a constant section of the pipe. When the airflow flows into the thread tube from nozzle needle exit f, the airflow of tube B is towed by the high speed airflow, weft can enter the thread tube from weft inlet D, and the weft is then accelerated in the thread tube. It is obvious that the functions of the nozzle needle are to accelerate airflow and make threading more convenient. The accelerated motion of weft is finished in the thread tube.

We divided the main nozzle into four parts called Tube A, Tube B, Tube C1, and Tube C2 which may be identified in Figure 1 by the following descriptions:

Tube A: a convergent-divergent nozzle outside of main nozzle needle.

Tube B: a converging nozzle inside the main nozzle needle.

Tube C1: from the nozzle needle tip ($x = 0$) to $x/D = 5$ where x is the length of the thread tubes. This tube may be regarded as an air ejector. (The $x/D = 5$ point is called the 'uniformly mixed flow point'.)

Tube C2: from the 'uniformly mixed flow point' ($x/D = 5$) to the thread tube exit. This tube is an adiabatic frictional cylindrical pipe.

Structure analysis of tube A and calculation of airflow parameters of the exit

This tube belongs to the convergent-divergent nozzle. For the air jet loom, we

considered the gas stagnation point of tube A to be the main tank. On the basis of the property of the one-dimensional isentropic compressible flow, the following relationships are obtained:

$$\left. \begin{aligned} V_{A2} &= \sqrt{\frac{2k}{k-1} RT_T \left[1 - \left(\frac{P_{A2}}{P_T} \right)^{\frac{k-1}{k}} \right]} \\ \frac{P_T}{P_{A2}} &= \left(1 + \frac{k-1}{2} M_{A2}^2 \right)^{\frac{k}{k-1}} \\ T_{A2} &= \frac{T_T}{1 + \frac{k-1}{2} M_{A2}^2} \\ c_{A2} &= \sqrt{kRT_{A2}} \\ \rho_{A2} &= \frac{P_{A2}}{RT_{A2}} \end{aligned} \right\} (1)$$

The airflow parameters of the exit can be calculated by the system of equations (1). Based on these calculations, we are able to state that the airflow speed at throat will obtain sonic velocity when the air pressure reaches 3 atm at the inlet. Based on the convergent principle, if we continue to increase the pressure supplied, the exit velocity cannot increase, it is equal to 1 Ma, and only the exit pressure increases. The ratio of the air exit pressure to the inlet pressure is 0.5283.

Structure analysis of tube B and airflow speed calculation

This tube may be regarded as a composite tube that consists of an isentropic flow-converging nozzle and a constant-section friction tube. Figure 2 shows an amplified schematic diagram. The airflow is accelerated in the converging tube, but its velocity cannot exceed the sonic velocity. Whether or not it reaches sonic velocity, it is along the length of the cylindrical tube. Before the airflow velocity reaches the sonic velocity, the air pressure of the exit is invariable, and always equals to the exit pressure of tube A. Here, the weft is pulled and enters the thread tube. On the basis of the theory of the constant-section adiabatic flow friction tube, the airflow velocity tends towards sonic velocity. For subsonic airflow in the inlet, the airflow is accelerated in the cylindrical tube. In contrast, for supersonic airflow in the inlet, the airflow is decelerated in the cylindrical tube.

Now we consider the cross section, which connects the converging tube and the cylindrical tube, as section 1; the parameters of section 1 are marked with the subscript 1. We consider the exit cross section as section 2; the parameters

of section 2 are marked with the subscript 2. According to the fundamental equation of fluid mechanics [7, 9], we obtain equation (2):

$$\frac{4\mu L_{T2}}{D_p} = \frac{1}{k} \left(\frac{1}{M_{B1}^2} - \frac{1}{M_{B2}^2} \right) + \frac{k+1}{2k} \ln \left(\frac{M_{B1}^2}{M_{B2}^2} \frac{1+(k-1)M_{B1}^2/2}{1+(k-1)M_{B2}^2/2} \right) \quad (2)$$

where: M_{B2} can be obtained through an analysis of tube C1, and so M_{B1} can be solved by numerical approximation [8].

Structure analysis of tube C1 and airflow parameters calculation of tube B exit

This tube can be regarded as an air ejector. The high velocity airflow from tube A elicits the airflow of tube B, and let weft into the thread tube without hindrance. On the basis of the continuity equation in unsteady flow, the mass flow ($\dot{m}_{C12} + \dot{m}_{B2}$) that flows into tube C1 should be equal to the mass flow (\dot{m}_{C12}) that flows out tube C1:

$$\dot{m}_{C12} = \dot{m}_{C12} + \dot{m}_{B2} \quad (3)$$

On the basis of momentum equation in unsteady flow, the sum of the intensity pressure resultant force and the momentum flux in tube C1 inlet should be equal to that of tube C1 exit:

$$(P_{A2}A_{A2} + \dot{m}_{A2}V_{A2}) + (P_{B2}A_{B2} + \dot{m}_{B2}V_{B2}) = P_{C12}A_{C12} + \dot{m}_{C12}V_{C12} \quad (4)$$

On the basis of energy equation in unsteady flow, the sum of enthalpy and kinetic energy flux in tube C1 inlet should be equal to that of tube C1 exit:

$$\dot{m}_{A2} \left(\frac{k}{k-1} \frac{P_{A2}}{\rho_{A2}} + \frac{V_{A2}^2}{2} \right) + \dot{m}_{B2} \left(\frac{k}{k-1} \frac{P_{B2}}{\rho_{B2}} + \frac{V_{B2}^2}{2} \right) = \dot{m}_{C12} \left(\frac{k}{k-1} \frac{P_{C12}}{\rho_{C12}} + \frac{V_{C12}^2}{2} \right) \quad (5)$$

Air parameters of the tube C1 exit can be obtained through an analysis of tube C2 by substituting them into equations (3) ~ (5), the air parameters of tube B exit can then be calculated.

Structure analysis of tube C2 and calculation of airflow parameters

This tube is a constant-section adiabatic flow friction tube (see Figure 1). We are able to test the exit velocity by the following experimentation, and then from the system of equations (6), the airflow parameters of tube C2 exit and the inlet speed of tube C2 can be calculated.

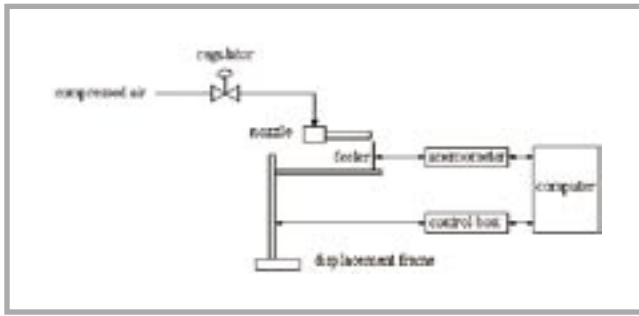


Figure 3. Schematic diagram of hot wire anemometer measuring speed.

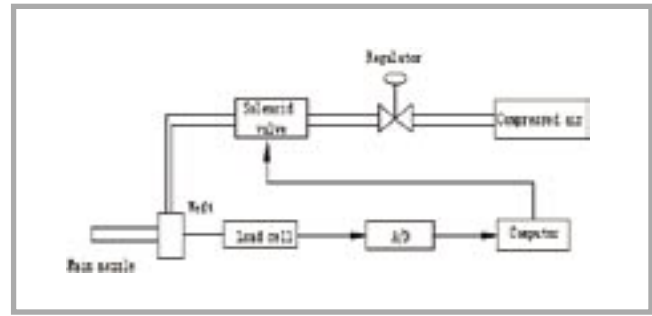


Figure 4. PF testing device.

Table 1. Airflow parameters of key points in main nozzle.

Air parameters of main tank	Pressure, Pa	150	200	220	250	280	300	320	350	380	400	430
	Mach number	0	0	0	0	0	0	0	0	0	0	0
	Temperature, K	296	296	296	296	296	296	296	296	296	296	296
	Speed, m/s	0	0	0	0	0	0	0	0	0	0	0
	Density, kg/m ³	1.766	2.354	2.590	2.943	3.296	3.531	3.767	4.120	4.473	4.709	5.062
Air parameters of tube A exit	Pressure, kPa	114.00	131.08	136.81	144.52	151.38	158.49	169.06	184.91	200.75	211.32	227.17
	Mach number	0.639	0.801	0.853	0.921	0.980	1	1	1	1	1	1
	Temperature, K	273.67	262.34	258.43	253.10	148.30	246.57	246.57	246.57	246.57	246.57	246.57
	Speed, m/s	211.78	260.05	274.73	293.59	309.55	314.76	314.76	314.76	314.76	314.76	314.76
	Density, kg/m ³	1.451	1.741	1.845	1.990	2.124	2.239	2.388	2.612	2.836	2.986	3.209
Air parameters of tube C2 exit	Pressure, kPa	101	101	101	101	101	101	101	101	101	101	101
	Mach number	0.457	0.608	0.661	0.746	0.791	0.826	0.853	0.896	0.928	0.951	1.000
	Temperature, K	284.13	275.62	272.22	266.36	263.08	260.08	258.40	255.05	252.51	250.66	246.67
	Speed, m/s	154.41	202.33	218.61	244.05	257.17	267.13	274.85	286.83	295.59	301.81	314.82
	Density, kg/m ³	1.242	1.281	1.297	1.326	1.342	1.355	1.366	1.384	1.398	1.408	1.431
Air parameters of tube C2 inlet	Pressure, kPa	117.77	133.83	141.04	154.62	162.52	169.11	174.65	183.54	190.67	196.07	207.45
	Mach number	0.395	0.467	0.484	0.503	0.510	0.514	0.516	0.519	0.520	0.520	0.521
	Temperature, K	287.04	283.63	282.75	281.75	281.37	281.15	281.04	280.87	280.82	280.82	280.76
	Speed, m/s	134.15	157.65	163.14	169.24	171.48	172.76	173.40	174.35	174.67	174.67	174.99
	Density, kg/m ³	1.430	1.644	1.738	1.912	2.013	2.096	2.165	2.277	2.366	2.433	2.575
Air parameters of tube B exit	Pressure, kPa	237.54	253.99	262.56	283.92	285.76	291.22	292.94	297.39	295.61	296.16	308.05
	Mach number	0.300	0.344	0.354	0.368	0.362	0.361	0.356	0.349	0.337	0.329	0.325
	Temperature, K	290.51	289.21	288.87	288.33	288.27	288.51	288.82	288.96	289.49	289.86	289.78
	Speed, m/s	102.66	117.34	120.53	125.35	123.32	122.93	121.15	118.95	114.86	112.15	110.77
	Density, kg/m ³	2.849	3.060	3.167	3.431	3.454	3.517	3.534	3.586	3.558	3.560	3.704
March number of tube B inlet		0.298	0.340	0.350	0.364	0.358	0.357	0.352	0.345	0.334	0.326	0.322

$$\left. \begin{aligned}
 \frac{4\mu_{C2}L_{C2}}{D_{C2}} &= \frac{1}{k} \left(\frac{1}{M_{C2}^2} - \frac{1}{M_{C2}^2} \right) + \\
 &= \frac{k+1}{2k} \ln \left(\frac{M_{C2}^2}{M_{C2}^2} \times \frac{1+(k-1)M_{C2}^2/2}{1+(k-1)M_{C2}^2/2} \right) \\
 T_{C2} &= T_1 - V_{C2}^2 / 2C_p \\
 P_{C2} &= P_{C2} / RT_{C2} \\
 \rho_{C2} &= \sqrt{kRT_{C2}} \\
 M_{C2} &= V_{C2} / c_{C2}
 \end{aligned} \right\} (6)$$

When airflow flows with subsonic velocity, an increase in the pressure supplied leads to an increase in the airflow velocity, and in the pressure of the thread tube. However, the exit pressure of tube C2 does not change; it is the same as atmospheric pressure. When an increase in the supplied pressure leads to the level of the exit pressure of tube C2 reaching sonic velocity, if we continued to increase in

the pressure supplied, then the exit velocity would not be able to increase, but instead the exit pressure would increase. Hence, the PF would also increase. Because the air jet loom always works at subsonic velocity, we consider the exit pressure of tube C2 to be constant. Similar to tube B, airflow is accelerated in the thread tube. Because tube C2 is longer than tube B, weft gets a larger PF in tube C2 than that of tube B.

An experiment with the air speed of tube C2 exit

In order to calculate the PF by using a derivational equation, we needed to know the Mach number which was found at the exit of nozzle. We used a hot wire anemometer to measure the airflow

speed in the tube C2 exit. The merits of the tester was the power of its function, quick to operate and with high precision. Here we adopted the IFA100 system of TSI, which includes a Model158 computer, Model150 speed measuring module, Model157 signal module, and Model140 temperature measuring module. Figure 3 shows its work principle.

Table 1 shows the measured/calculated results of airflow parameters in the main nozzle with different pressure supplied. In this experiment, the testing conditions were as follows:

$$\begin{aligned}
 D_C &= 0.004 \text{ m}, & L_C &= 0.22 \text{ m} \\
 \mu_C &= 0.004 & D_B &= 0.0025 \text{ m} \\
 L_B &= 0.022 \text{ m} & \mu_B &= 0.0025 \\
 P_0 &= 1.01 \times 10^5 \text{ Pa} \\
 C_p &= 1004.6 \text{ J/kg} \cdot \text{K}.
 \end{aligned}$$

Table 2. Diameter and air-drag coefficient.

Yarn	d (× 10 ⁴ m)	ρ _f
13 tex cotton	1.395	0.026
13×2 tex T/C	1.881	0.033

Dynamics analysis of weft insertion in main nozzle

We chose a random tiny yarn of length dl , and considered the weft movement along axis. The PF of the tiny yarn was [10]:

$$dF = 1/2 \rho_f \rho \pi d (v-u)^2 dl \quad (7)$$

where:

- F - the PF,
- ρ_f - air-drag coefficient,
- ρ - the airflow density,
- d - the yarn diameter,
- v - the airflow velocity,
- u - the yarn velocity,
- l - the yarn length in the main nozzle.

Because the main nozzle is short, we should consider that ρ_f was a constant and ρ_f did not change with the air veloc-

ity. Based on atomic formulas of gas dynamics, the PF had been analysed in a former paper [11]. For equation (7), we adopted symbolic integration and as the integrating range is $[M_1, M_2]$, we obtain the integrated function as follows:

$$F = \frac{\pi d D \rho_f}{4 \mu R k} \frac{P_2 M_2}{(1 - M_2^2 c^2 / 2 C_p)} [\Phi_{i1} - \Phi_{i2}] \quad (8)$$

here:

$$\Phi_i = (1+k) \gamma \ln(M_i) + (0.5(1+k) \gamma^2 - c^2) M_i + c \gamma / M_i^2 - u^2 / 3 M_i^2 - 0.5(1+k) \gamma \ln(1 + M_i / \sqrt{5}) - \sqrt{5} \arctan(M_i / \sqrt{5}) - (0.5(1+k) \gamma^2 - 0.5(1+k) \gamma - 0.1(1+k) \gamma^2)$$

where:

- $i = 1, 2$,
- P_2 - the pressure of nozzle exit,
- M_1 - the Mach number of inlet,
- M_2 - the Mach number of exit,
- D - the inner diameter of main nozzle,
- c - the sonic velocity.

Because tube C1 is short, the pull force in tube C1 is ignored. The PF can be divided into force $F1$ in the friction tube of

tube B and force $F2$ in the friction tube of tube C2:

$$F = F1 + F2 \quad (9)$$

From equation (8), the force $F1$ can be obtained. In contrast, the air inlet velocity of tube C2 was unknown. So, in order to obtain the solution of $F2$, we had to do some experiments to obtain its velocity.

Results and discussion

We designed the experiment method as follows (see Figure 4): compressed air passed the regulating valve, and the gas entered the main nozzle through a solenoid valve by computer control. One side of the weft extended into the main nozzle, and another connected with the load cell. The signal was sent to computer via A/D converter which saved and processed the data. Because the initial velocity of the yarn was equal to zero, the tested tension was the beginning of weft insertion.

The experiment tested the pull force of two types of yarns under different conditions. Table 2 shows the diameter and air-drag coefficient. Following from equation (9), the PF can be calculated.

The supplied pressure was an important craft parameter of weft insertion. An increase in supplied pressure leads to an increase in airflow velocity. Table 3 shows the measured and calculated results of the pull force at different pressures. Figure 5 shows the curve of the measured and calculated results with cotton yarn and Tencel/cotton yarn. From the diagrams, it can be seen that the calculations agree with the observations, so equation (8) is able to reflect the influence of air velocity on the PF. An increase in airflow velocity leads to an increase in the PF. Furthermore, as may be seen in Table 3, the PF emerging from tube B predominated when the pressure supplied is low; however, the PF that emerges from tube C predominated when the supplied pressure exceeded 0.2Mpa; in such a case the pull force of tube B would be constant. From the results calculated, we can see that the pull force of tube B was much smaller than that of tube C2. Thus the pull force of the thread tube was dominant.

Conclusions

Based on the analytical and experimental investigations presented in this paper, the following conclusions can be drawn:

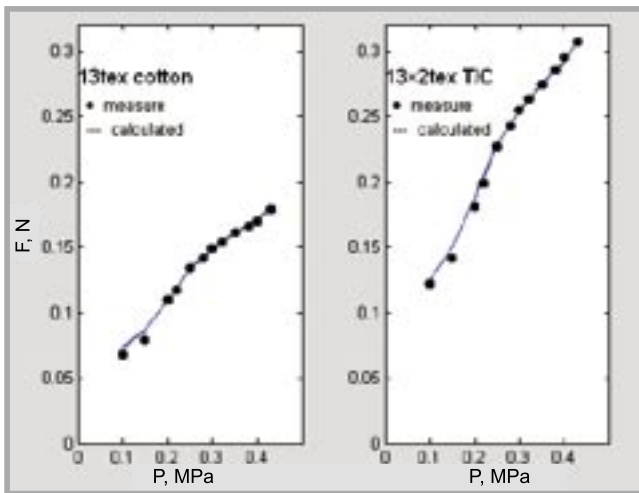


Figure 5. The relation between supplied pressure and PF.

Table 3. The measured value and calculated value of pull force with different pressure.

Supplied pressure (10 ⁶ Pa)	13 tex cotton				13×2 tex T/C			
	Calculate, N			Measure, N	Calculate, N			Measure, N
	F2	F1	F	F	F2	F1	F	F
0.15	0.0330	0.0033	0.0363	0.038	0.0564	0.0056	0.0620	0.071
0.20	0.0574	0.0059	0.0633	0.065	0.0982	0.0101	0.1083	0.111
0.22	0.0673	0.0058	0.0731	0.074	0.1152	0.0099	0.1251	0.132
0.25	0.0847	0.0060	0.0907	0.093	0.1450	0.0103	0.1553	0.161
0.28	0.0992	0.0062	0.1054	0.106	0.1670	0.0106	0.1776	0.182
0.30	0.1024	0.0063	0.1087	0.110	0.1752	0.0108	0.1860	0.195
0.32	0.1086	0.0065	0.1151	0.121	0.1859	0.0111	0.1970	0.203
0.35	0.1185	0.0068	0.1253	0.127	0.2028	0.0116	0.2144	0.221
0.38	0.1265	0.0052	0.1317	0.133	0.2165	0.0089	0.2254	0.232
0.40	0.1326	0.0054	0.1380	0.139	0.2269	0.0092	0.2361	0.241
0.43	0.1447	0.0057	0.1504	0.152	0.2476	0.0098	0.2574	0.263

- The structure of the main nozzle and its working accuracy are important to the pull force (PF). Decreasing the diameter of the main nozzle can reduce energy consumption; whereas increasing the length of the thread tube can increase the PF. As the trend of airjet loom movements is towards high speed, the main nozzle should be the main subject of future research.
- The inlet of the thread tube is a bottleneck of the main nozzle, where the air speed decreases very rapidly.
- There may be some errors in the experiment data, but the general tendency is correct. Because the air velocity at the exit needs to be measured yielding data for the calculation of theories, the pull force still cannot be determined according to the structure size of nozzle only.



References

1. Adanur S., Bakhtiyarov S.; *Analysis of Air-flow in Single Nozzle Air-Jet Filling Insertion: Corrugated Channel Model*, *Textile Res. J.* Vol. 66 (1996) pp. 401-406.
2. Sadasuke F. K.; *Flow characteristics in weft-acceleration pipe of air-jet loom*, *J. Text. Mach. Soc.* Vol. 38 (1992) pp. 95-100.
3. Kirubakaran B., Srivastava, T. V. K.; *Air-Jet Weft Insertion*, *Ind. Textile J.* Vol. 109 (1998) pp. 10-12.
4. Nihat C., Osman B.; *A Mathematical Model for Numerical Simulation of Weft Insertion On an Air-Jet Weaving Machine*, *Textile Res. J.* Vol. 74 (2004) pp. 236-240.
5. Oh T.H., Kim S. D., Song D. J.; *A Numerical Analysis of Transonic/Supersonic Flows in the Axisymmetric Main Nozzle of an Air-jet Loom*, *Textile Res. J.* Vol. 71 (2001) pp. 783-790.
6. Yan H. Q., Dai J. G.; *Principle and Application of air jet loom*, (China textile publishing house, Beijing), 1996.
7. Ying R. S., Zhang M. Y.; *Hydromechanics*, (Xi'an jiaotong university publishing house, Xi'an), 2001, pp. 246-249.
8. Zhang Z. Y., Xu Y. Q.; *MATLAB Lesson*, (Beijing aviation & astronautics university publishing house, Beijing), 2001, pp. 108-109.
9. Douglas J. F., Gasiorek J. M.; *Hydro-mechanics*, (High education publishing house, Beijing), 2000, pp. 299-318.
10. Cao R.; *Air-jet filling*, (Textile industry publishing house, Beijing), 1984, pp. 9-10.
11. Shen D. F., Ye G. M.; *Dynamics analysis on pneumatic weft insertion*, *Silk Monthly*. Vol. 6 (2006) pp. 29-33.

■ Received 29.03.2006 Reviewed 20.09.2007

UNIVERSITY OF BIELSKO-BIAŁA

Faculty of Materials and Environmental Sciences

The Faculty was founded in 1969 as the Faculty of Textile Engineering of the Technical University of Łódź, Branch in Bielsko-Biała. It offers several courses for a Bachelor of Science degree and a Master of Science degree in the field of Textile Engineering and Environmental Engineering and Protection. The Faculty considers modern trends in science and technology as well as the current needs of regional and national industries. At present, the Faculty consists of:

■ The Institute of Textile Engineering and Polymer Materials, divided into the following Departments:

- Physics and Structural Research
- Textiles and Composites
- Physical Chemistry of Polymers
- Chemistry and Technology of Chemical Fibres

■ The Institute of Engineering and Environmental Protection, divided into the following Departments:

- Biology and Environmental Chemistry
- Hydrology and Water Engineering
- Ecology and Applied Microbiology
- Sustainable Development of Rural Areas
- Processes and Environmental Technology



University of Bielsko-Biała
Faculty of Materials and Environmental Science

ul. Willowa 2, 43-309 Bielsko-Biała
tel. +48 33 8279 114, fax. +48 33 8279 100